

LETTERS

Restoration of p53 function leads to tumour regression *in vivo*

Andrea Ventura^{1*}, David G. Kirsch^{1,2*}, Margaret E. McLaughlin¹, David A. Tuveson¹, Jan Grimm³, Laura Lintault¹, Jamie Newman¹, Elizabeth E. Reczek¹, Ralph Weissleder³ & Tyler Jacks^{1,4}

Tumorigenesis is a multi-step process that requires activation of oncogenes and inactivation of tumour suppressor genes¹. Mouse models of human cancers have recently demonstrated that continuous expression of a dominantly acting oncogene (for example, *Hras*, *Kras* and *Myc*) is often required for tumour maintenance^{2–5}; this phenotype is referred to as oncogene addiction⁶. This concept has received clinical validation by the development of active anticancer drugs that specifically inhibit the function of oncoproteins such as BCR-ABL, c-KIT and EGFR^{7–10}. Identifying additional gene mutations that are required for tumour maintenance may therefore yield clinically useful targets for new cancer therapies. Although loss of p53 function is a common feature of human cancers¹¹, it is not known whether sustained inactivation of this or other tumour suppressor pathways is required for tumour maintenance. To explore this issue, we developed a Cre-*loxP*-based strategy to temporally control tumour suppressor gene expression *in vivo*. Here we show that restoring endogenous p53 expression leads to regression of autochthonous lymphomas and sarcomas in mice without affecting normal tissues. The mechanism responsible for tumour regression is dependent on the tumour type, with

the main consequence of p53 restoration being apoptosis in lymphomas and suppression of cell growth with features of cellular senescence in sarcomas. These results support efforts to treat human cancers by way of pharmacological reactivation of p53.

Biochemical and genetic studies have demonstrated that p53 responds to genotoxic and oncogenic stresses by inducing cell cycle arrest or apoptosis¹¹. Because oncogenic stress can persist after p53 inactivation, loss of p53 function may not only play a role in the early stages of tumour development, but also be required for the continued proliferation or survival of an established tumour^{12–14}. To test this hypothesis, we used a genetic strategy to restore endogenous p53 expression in primary, autochthonous tumours. Mice carrying a reactivatable p53 knockout allele were generated by inserting a transcription-translation stop cassette flanked by *loxP* sites (LSL) in the first intron of the endogenous wild-type p53 locus (Fig. 1a, b). When in place, the STOP cassette efficiently prevents expression of the p53 gene (Fig. 1c, d). Cells from homozygous *p53*^{LSL/LSL} (referred to hereafter as p53-LSL) mice are functionally equivalent to p53 null (*p53*^{−/−}) cells, as demonstrated by the absence of cell-culture-induced senescence (Fig. 1e) and by their marked genetic instability

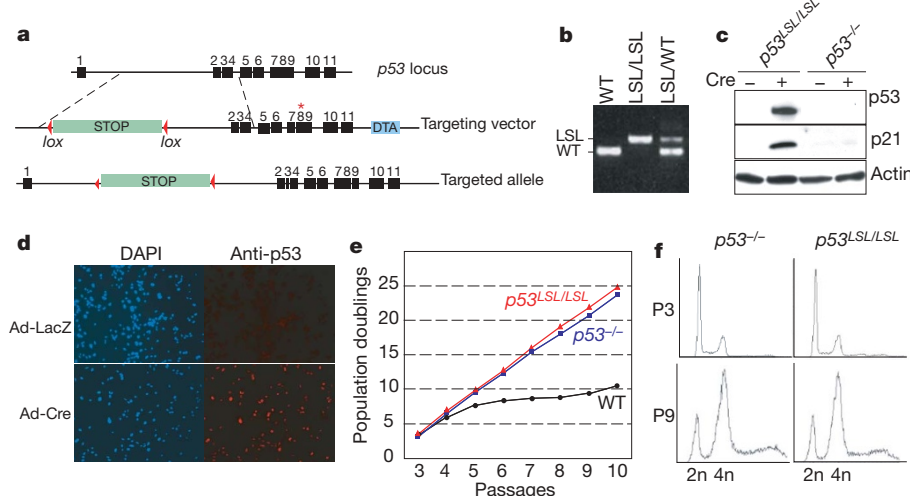


Figure 1 | Generation of the p53-LSL allele. **a**, The p53-LSL allele was generated while engineering a point-mutant p53 allele³¹ when homologous recombination occurred between the LSL cassette and the point mutation (asterisk). **b**, Genotyping of p53-LSL mice by PCR (polymerase chain reaction) amplification of tail DNA. **c**, Western blot of passage 5 MEFs infected with empty or Cre-expressing recombinant adenoviruses

(Adeno-empty and Adeno-Cre). **d**, Anti-p53 immunostaining of *p53*^{LSL/LSL} (that is, p53-LSL) MEFs infected with Adeno-LacZ or Adeno-Cre and then treated with doxorubicin (0.2 µg ml^{−1}; 13 h). DAPI, 4,6-diamidino-2-phenylindole. **e**, 3T protocol on *p53*^{LSL/LSL}, *p53*^{−/−} and wild-type (WT) MEFs. **f**, DNA content of early (P3) and late (P9) passage *p53*^{LSL/LSL} or *p53*^{−/−} MEFs. Diploid (2n) and tetraploid (4n) DNA content is indicated.

¹Center for Cancer Research, Massachusetts Institute of Technology, Cambridge, Massachusetts 02142, USA. ²Department of Radiation Oncology, ³Center for Molecular Imaging Research, Massachusetts General Hospital, Boston, Massachusetts 02129, USA, and Harvard Medical School, Boston, Massachusetts 02115, USA. ⁴Howard Hughes Medical Institute, Chevy Chase, Maryland 20815, USA.

*These authors contributed equally to this work.

(Fig. 1f). However, owing to the presence of flanking *loxP* sites, the STOP cassette can be excised by the Cre recombinase¹⁵, thus restoring expression of the endogenous *p53* gene (Fig. 1c, d). Because mice lacking *p53* are tumour-prone^{16,17}, this system offers an opportunity to study the consequences of *p53* reactivation in primary tumours *in vivo*.

To temporally control *p53* reactivation *in vivo*, we have also generated mice carrying a Cre-recombinase-Oestrogen-Receptor-T2 (Cre-ER^{T2}) allele targeted to the ubiquitously expressed ROSA26 locus (Supplementary Fig. 1a, b). The ER^{T2} moiety retains the Cre recombinase in the cytoplasm until tamoxifen administration releases this inhibition¹⁸, thus permitting the recombination of genomic *loxP* sites. Efficient tamoxifen-induced Cre-mediated recombination throughout the body was demonstrated by crossing Cre-ER^{T2} mice to mice carrying a Cre-responsive β-galactosidase reporter allele¹⁹ (Supplementary Fig. 1c).

Next, Cre-ER^{T2} and *p53*-LSL mice were crossed to generate cohorts of *p53*-LSL homozygous mutant animals carrying the Cre-ER^{T2} allele (*p53*^{LSL/LSL};Cre-recombinase-Oestrogen-Receptor-T2, hereafter referred to as *p53*-LSL;Cre-ER^{T2}) as well as *p53*-LSL homozygotes without the Cre-ER^{T2} allele (hereafter referred to as *p53*-LSL). To accelerate tumour formation, some of these mice were irradiated shortly after birth, as radiation decreases tumour latency in *p53* null mice²⁰. These animals underwent periodic magnetic resonance imaging (MRI) to detect the presence of cancer (Fig. 2a). After tumour detection, the mice were treated with tamoxifen and then re-imaged at different times thereafter.

As shown in Fig. 2, in the majority of *p53*-LSL;Cre-ER^{T2} mice, tamoxifen treatment caused regression of autochthonous lymphomas and sarcomas (Fig. 2b, c, f; Supplementary Fig. 2, Supplementary Movies). This effect was due to *p53* reactivation rather than tamoxifen treatment alone, because in Cre-ER^{T2}-negative *p53*-LSL mice, tumours rapidly progressed despite treatment (Fig. 2d–f). Figure 2f summarizes the responses observed in the animals studied. Out of 10

Cre-ER^{T2}-positive tumours treated (6 thymic lymphomas, 3 sarcomas and 1 intra-abdominal lymphoma), 7 showed regression ranging from 46% to 100%. In two tumours (a thymic lymphoma and an osteosarcoma), tamoxifen prevented tumour progression but failed to decrease the size of the neoplasia (Fig. 2f; Supplementary Fig. 3). In one thymic lymphoma tumour progression was observed despite tamoxifen treatment (Fig. 2f; Supplementary Fig. 3). DNA and immunohistochemical analysis indicated that in this case resistance to tamoxifen was due to the specific deletion of the Cre-ER^{T2} allele in the tumour (Supplementary Fig. 3e, f). In contrast, all Cre-ER^{T2}-negative tumours (two thymic lymphomas, two abdominal lymphomas and three sarcomas) progressed despite tamoxifen administration (Fig. 2d–f). These results demonstrate that sustained *p53* inactivation is required for tumour maintenance in autochthonous lymphomas and sarcomas in the mouse.

To study the mechanisms responsible for tumour regression, tumours from *p53*-LSL;Cre-ER^{T2} mice were analysed 24 or 48 h after tamoxifen treatment. In thymic lymphomas, tumour regression was already apparent at 48 h (approximately 75% reduction in tumour volume; see Fig. 3a). In addition, *p53* expression was detectable as early as 24 h following tamoxifen treatment and was associated with widespread apoptosis (Fig. 3b). We next derived three thymic lymphoma cell lines, two from *p53*^{LSL/+};Cre-ER^{T2} mice and one from a *p53*-LSL;Cre-ER^{T2} mouse. An additional line, to be used as a control, was derived from a thymic lymphoma arising in a *p53*^{+/−} mouse. In all cases, *p53* expression was undetectable by western blot (data not shown), suggesting that in the tumours arising in *p53*^{LSL/+} and *p53*^{+/−} mice expression of the wild-type *p53* allele had been lost. 4-hydroxytamoxifen (4-OHT) treatment caused cell death in the *p53*-LSL;Cre-ER^{T2}-positive cell lines but not in the control cells (Fig. 3c). A time-course experiment with the *p53*-LSL;Cre-ER^{T2} thymic lymphoma cell line showed that cell death began within 12 h after 4-OHT administration and was virtually complete by 96 h (Fig. 3d). Moreover, just as the primary thymic lymphomas showed apoptotic

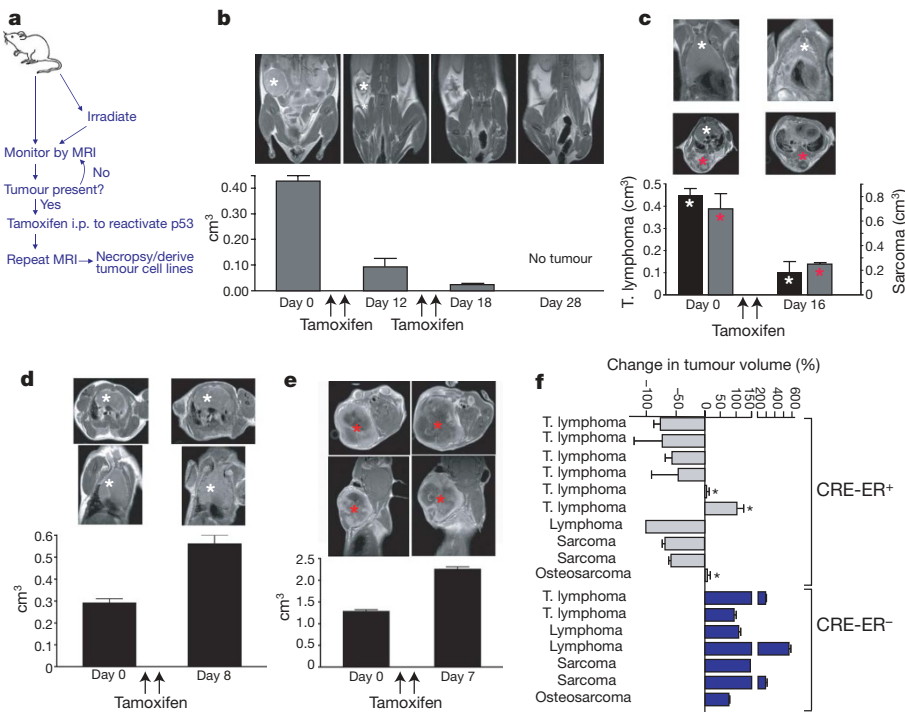


Figure 2 | p53 restoration leads to tumour regression in vivo. **a**, Flow chart of the strategy used to determine tumour response. i.p., intraperitoneal. **b–d**, MRI images (top) and tumour volumes (bottom) of *p53*-LSL;Cre-ER^{T2} (**b**, **c**) and *p53*-LSL (**d**, **e**) mice in response to tamoxifen (arrows). The tumours (asterisks) were an abdominal lymphoma (**b**), two thymic lymphomas (t. lymphoma; **c** and **d**, white asterisks) and two sarcomas (**c** and

e, red asterisks). The volumes were calculated from the available MRI sequences ($n = 2$ to 6) for each time point, and are shown as mean \pm 1 s.d. **f**, Summary of maximal responses to tamoxifen of tumours from Cre-ER^{T2}-positive (grey bars) and Cre-ER^{T2}-negative (blue bars) mice. Asterisks indicate tumours from Cre-ER^{T2}-positive mice with limited or no response (see also Supplementary Fig. S3).

cell death (Fig. 3b), immunoblot for activated caspase-3 and flow-cytometry analysis of annexin-5 positive cells (Fig. 3e and data not shown) demonstrated that apoptosis was the primary consequence of p53 reactivation in this context. Interestingly, the cell cycle distribution of the viable lymphoma cells did not change in response to 4-OHT administration (Fig. 3e), despite induction of the p21 cyclin-dependent kinase inhibitor (data not shown).

Compared to lymphomas, sarcoma regression upon tamoxifen treatment was more delayed, with only a modest reduction at 48 h (Fig. 4a). Furthermore, although p53 was clearly expressed in the sarcomas at 24 and 48 h (Fig. 4b and data not shown) extensive apoptosis was not evident at these time points (Fig. 4b). Despite the absence of a clear increase in apoptosis, prolonged tamoxifen treatment led to regression of sarcomas (Fig. 2c, f; Supplementary Figs 4 and 5), with the residual mass largely composed of necrotic tissue (Supplementary Fig. 5). In order to determine the mechanism underlying sarcoma regression, we investigated the consequences of p53 restoration in two cell lines derived from p53-LSL sarcomas.

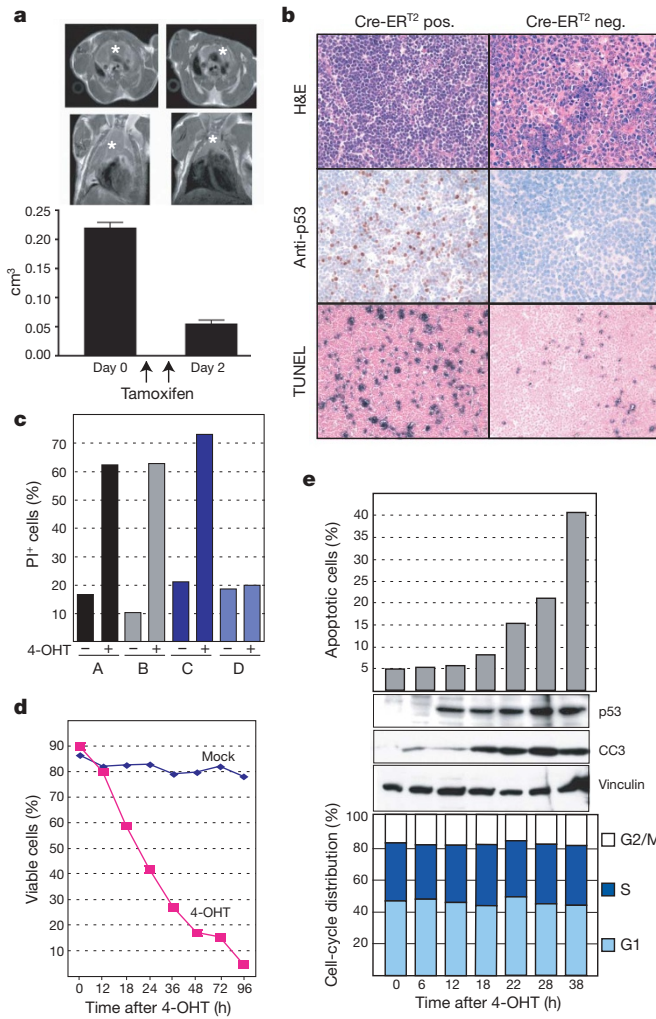


Figure 3 | p53 restoration in lymphomas leads to apoptosis. **a**, MRI images (top) and tumour volumes (bottom) of a p53-LSL;Cre-ER^{T2} lymphoma. Error bars, ± 1 s.d. **b**, p53 immunohistochemistry and TUNEL staining in thymic lymphomas after tamoxifen treatment. H&E, haematoxylin and eosin. **c**, Viability of thymic lymphoma cell lines derived from Cre-ER^{T2}-positive mice (lines A–C), and a p53^{+/-} mouse (line D) treated with vehicle (ethanol) or 250 nM 4-OHT for 48 h. Dead cells were identified by their retention of propidium iodide (PI+). **d**, Time course of cell viability of line A treated with vehicle (mock) or 250 nM 4-OHT. **e**, Line A was treated with 4-OHT and analysed for apoptosis (annexin V staining, top panel), expression of p53, cleaved caspase 3 (CC3) and vinculin (western blots, middle panel) and cell cycle distribution (PI staining, bottom panel).

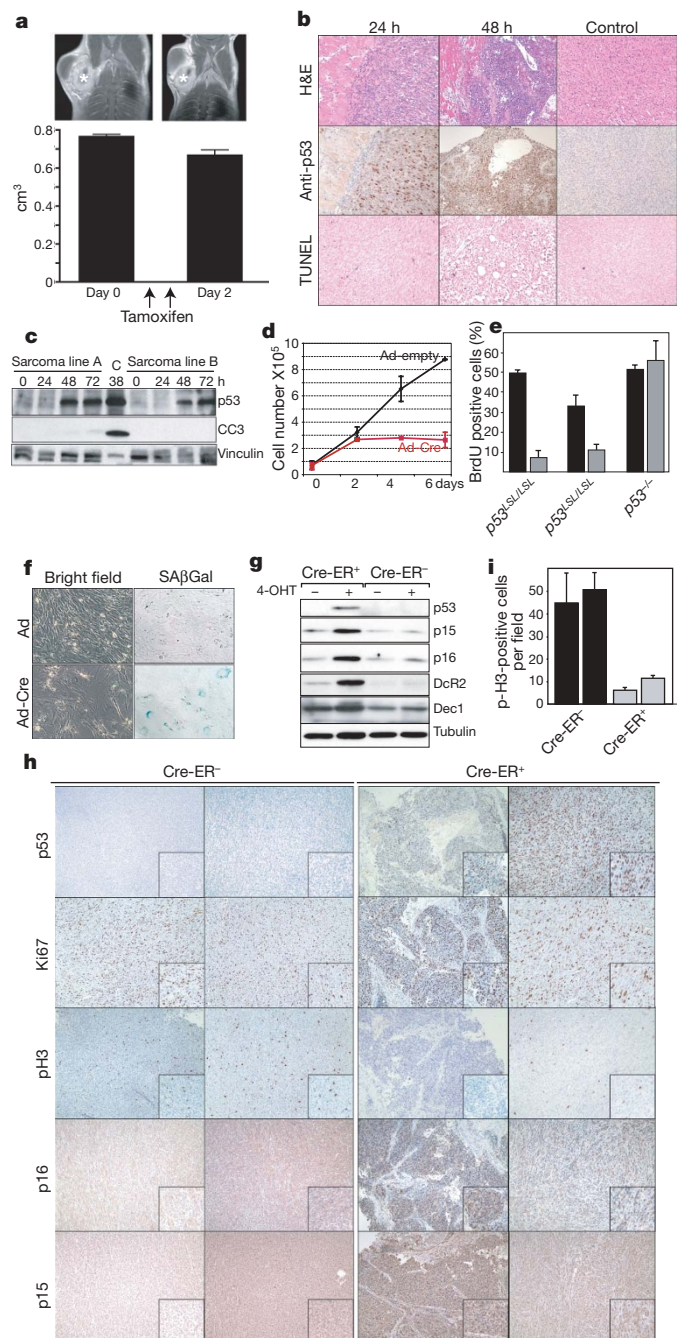


Figure 4 | p53 restoration in sarcomas leads to growth suppression with features of cellular senescence. **a**, MRI images (top) and tumour volumes (bottom) of a p53-LSL;Cre-ER^{T2} soft tissue sarcoma (STS). Error bars, ± 1 s.d. **b**, p53 immunohistochemistry and TUNEL staining of p53-LSL;Cre-ER^{T2} STSs after tamoxifen treatment. The control is a Cre-ER^{T2}-negative sarcoma. **c**, p53-LSL sarcoma cells were infected with Adeno-Cre and harvested for immunoblot. Lane C, positive control for cleaved caspase 3. **d**, Proliferation assay. Average of two independent cell lines ± 1 s.d. is shown. **e**, BrdU (5-bromodeoxyuridine) incorporation in sarcoma cells infected with Adeno-GFP (black bars) or Adeno-Cre-GFP (grey bars). Error bars, ± 1 s.d. **f**, Senescence-associated β -galactosidase (SA β Gal) staining of a sarcoma cell line 5 days after infection with Adeno-empty or Adeno-Cre. **g**, Immunoblot analysis of senescence markers in p53-LSL;Cre-ER^{T2} and p53-LSL sarcoma cells 11 days after 4-OHT tamoxifen treatment. **h**, Immunohistochemistry analysis of four sarcomas 5–6 days after *in vivo* tamoxifen administration. **i**, Quantification of phospho-histone H3 positive cells in sarcomas from **h**. Average of seven random 40 \times fields ± 1 s.d.

Consistent with the results *in vivo*, expression of Cre recombinase in these cell lines failed to induce significant apoptosis (Fig. 4c). Instead, restoration of p53 expression suppressed proliferation (Fig. 4d) and induced cell cycle arrest (Fig. 4e). In addition, these cells lost their spindle morphology, appeared flat and enlarged, and many of them expressed senescence-associated β -galactosidase (Fig. 4f).

Recent work has led to the identification of a number of proteins whose expression is increased in senescent pre-neoplastic lesions²¹. These markers include the cdk-inhibitors p15-Ink4b and p16-Ink4a, as well as Dcr2 and Dec1. We examined their expression in sarcoma cell lines derived from p53-LSL;Cre-ER^{T2} and p53-LSL mice. Only the Cre-ER^{T2}-positive sarcoma cells induced p15-Ink4b, p16-Ink4a, Dcr2 and (to a lesser extent) Dec-1 in response to tamoxifen treatment (Fig. 4g). We next examined whether cell cycle arrest and senescence markers are similarly induced by p53 restoration in sarcomas *in vivo*. Senescence-associated β -galactosidase positive cells were observed in one out of three Cre-ER^{T2}-positive sarcomas treated with tamoxifen for 5–6 days, but in none of the Cre-ER^{T2}-negative controls (Supplementary Fig. S6, and data not shown). Consistent with the data obtained in sarcoma cell lines, p15-Ink4b and p16-Ink4a expression was higher in the tamoxifen-treated Cre-ER^{T2}-positive sarcomas, compared to the Cre-ER^{T2}-negative ones (Fig. 4h). Although Ki67 staining was not significantly different after p53 restoration in these tumours, an analysis of phospho-histone H3 revealed a markedly lower fraction of proliferation in the tamoxifen-treated Cre-ER^{T2}-positive sarcomas (Fig. 4h and i). Taken together, these results indicate that the main consequence of p53 restoration in sarcomas is cell cycle arrest with some features of senescence. We did not observe upregulation of all senescence markers in every sarcoma studied *in vivo*, which may reflect the genetic and histological heterogeneity between the spontaneous mesenchymal tumours analysed here and epithelial pre-neoplastic lesions reported by others²¹. Furthermore, owing to the relatively low incidence of sarcomas in p53 null animals, our analysis of senescence markers *in vivo* has been relatively limited to date. We anticipate that with further studies of p53 restoration in sarcomas, we will be able to clarify the arrest/senescent phenotype of different sarcoma subtypes more fully.

Although tamoxifen treatment of p53-LSL;Cre-ER^{T2} mice leads to excision of the STOP cassette in both neoplastic and normal tissues, expression of the p53 protein was detectable by immunohistochemistry only in tumour cells (Figs 3b and 4b, and data not shown). Furthermore, histopathological analysis revealed no signs of p53-mediated toxicity in normal organs after acute p53 reactivation (data not shown). These results indicate that in p53 null mice, transformed cells are uniquely primed to stabilize and activate p53. In established tumours, one potential stimulus for p53 protein stabilization and activation is persistent oncogenic stress. Because the tumour suppressor gene *p19^{Arf}* is induced in response to oncogenic stimuli and is a well known activator of p53 (ref. 22), we analysed its expression levels in tumours from p53-LSL animals. Strikingly, high *p19^{Arf}* expression was frequently observed in both lymphomas and sarcomas but not in the normal tissues analysed (Supplementary Fig. 7 and data not shown). These results suggest that in lymphomas and sarcomas, *p19^{Arf}* might prime tumour cells to respond to p53 reactivation.

In this study, we have used a novel genetic strategy for restoring endogenous p53 activity in cells and in mice. By combining a reactivatable loss-of-function p53 allele together with a temporally regulated Cre recombinase, we demonstrate that sustained inactivation of p53 is required for the maintenance of primary, autochthonous lymphomas and sarcomas. This approach may be of general application for the study of other tumour suppressor gene pathways.

Interestingly, the mechanism of tumour regression after p53 restoration appears to be tumour type specific. In lymphomas, restoration of p53 caused widespread apoptosis, whereas the major consequence of p53 reactivation in sarcomas was cell cycle arrest with

features of cellular senescence. Because sarcomas also regressed following p53 reactivation *in vivo*, it is possible that senescent cells are rapidly cleared from the tumour mass. This hypothesis is consistent with results obtained in a mouse model of liver cancer in an accompanying paper²³. Alternatively, sarcoma regression may be a consequence of p53-dependent effects on tumour vasculature^{24,25} or on other stromal components. The effect is also tumour specific in that normal cells appeared not to respond to p53 reactivation. Thus, this represents an extremely promising anticancer strategy with a broad therapeutic window.

These results are also consistent with work in other model systems. For example, mouse embryo fibroblasts (MEFs) transformed by ectopically expressing an oncogenic *K-Ras* allele in the setting of doxycycline-regulated p53 knock-down enter senescence upon restoration of p53 expression²⁶. Tumours obtained by injecting these cells into nude mice also regressed in response to doxycycline treatment²⁶. Likewise, immortalized MEFs from a p53-oestrogen-receptor(tamoxifen) fusion knock-in mouse strain undergo senescence after treatment with tamoxifen²⁷, and temporarily activating p53 in these mice delays tumour development²⁸.

Owing to the prevalence of p53 pathway inactivation in human cancers, several pharmacological strategies aimed at restoring p53 function have been proposed. These include small molecules that restore point-mutant p53 proteins to a transcriptionally competent conformation¹³, as well as compounds that interfere with the Mdm2-p53 interaction²⁹ and gene-therapy-based approaches aimed at introducing a wild-type copy of the p53 gene into tumour cells³⁰. Provided that human cancers, like the mouse cancers studied here, remain dependent on sustained p53 inactivation for tumour maintenance, our results lend strong support to such therapeutic efforts.

METHODS

A detailed description of materials and methods is given in Supplementary Information.

Generation of p53-LSL mice. The p53-LSL allele was obtained as a by-product of our efforts to generate a R270H point mutant p53 allele³¹. All p53 exons and intron-exon boundaries were sequenced to ensure the absence of mutations. Oligonucleotide sequences for genotyping are available on request.

Generation of R26-Cre-ER^{T2} mice. A plasmid containing the Cre-ER^{T2} complementary DNA (pCre-ER^{T2}) was obtained from the laboratory of P. Chambon¹⁹. This cDNA was targeted to the ROSA26 locus as described in detail in the Supplementary Information.

Tamoxifen treatment. All animal studies and procedures were approved by the MIT Institutional Animal Care and Use Committee, and by the Subcommittee on Research Animal Care at Massachusetts General Hospital. Mice were of a mixed 129Sv/Jae and C57/B6 background. After detecting a tumour by MRI, mice were treated with tamoxifen (Sigma) by intraperitoneal injection. 100 μ l of tamoxifen (10 mg ml⁻¹ in corn oil) was injected every two to three days. Follow-up MRI was generally obtained 7–10 days after the first tamoxifen treatment.

MRI and tumour volume analysis. All animals were sequentially imaged using a 4.7 T Bruker Pharmascan (Bruker BioSpin) to screen for tumour growth and treatment response to tamoxifen. Tumour volume measurements were performed using T1- and T2-weighted coronal and axial image stacks. The tumours were manually segmented using Amira software (TGS) to obtain the tumour volume in cm³. For each time point, all measurements from the available sequences were used to calculate a mean volume \pm standard deviation in order to limit errors due to the manual segmentation process.

Received 26 September; accepted 13 December 2006.

Published online 24 January 2007.

1. Hanahan, D. & Weinberg, R. A. The hallmarks of cancer. *Cell* 100, 57–70 (2000).
2. Chin, L. *et al.* Essential role for oncogenic Ras in tumour maintenance. *Nature* 400, 468–472 (1999).
3. Jain, M. *et al.* Sustained loss of a neoplastic phenotype by brief inactivation of MYC. *Science* 297, 102–104 (2002).
4. Fisher, G. H. *et al.* Induction and apoptotic regression of lung adenocarcinomas by regulation of a *K-Ras* transgene in the presence and absence of tumor suppressor genes. *Genes Dev.* 15, 3249–3262 (2001).
5. Pelengaris, S., Khan, M. & Evan, G. I. Suppression of Myc-induced apoptosis in β cells exposes multiple oncogenic properties of Myc and triggers carcinogenic progression. *Cell* 109, 321–334 (2002).

6. Weinstein, I. B. Cancer. Addiction to oncogenes—the Achilles heel of cancer. *Science* **297**, 63–64 (2002).
7. Druker, B. J. et al. Efficacy and safety of a specific inhibitor of the BCR-ABL tyrosine kinase in chronic myeloid leukemia. *N. Engl. J. Med.* **344**, 1031–1037 (2001).
8. Demetri, G. D. et al. Efficacy and safety of imatinib mesylate in advanced gastrointestinal stromal tumors. *N. Engl. J. Med.* **347**, 472–480 (2002).
9. Lynch, T. J. et al. Activating mutations in the epidermal growth factor receptor underlying responsiveness of non-small-cell lung cancer to gefitinib. *N. Engl. J. Med.* **350**, 2129–2139 (2004).
10. Paez, J. G. et al. EGFR mutations in lung cancer: correlation with clinical response to gefitinib therapy. *Science* **304**, 1497–1500 (2004).
11. Sherr, C. J. Principles of tumor suppression. *Cell* **116**, 235–246 (2004).
12. Olivier, M. et al. The IARC TP53 database: new online mutation analysis and recommendations to users. *Hum. Mutat.* **19**, 607–614 (2002).
13. Bykov, V. J. et al. Restoration of the tumor suppressor function to mutant p53 by a low-molecular-weight compound. *Nature Med.* **8**, 282–288 (2002).
14. Snyder, E. L., Meade, B. R., Saenz, C. C. & Dowdy, S. F. Treatment of terminal peritoneal carcinomatosis by a transducible p53-activating peptide. *PLoS Biol.* **2**, E36 (2004).
15. Branda, C. S. & Dymecki, S. M. Talking about a revolution: The impact of site-specific recombinases on genetic analyses in mice. *Dev. Cell* **6**, 7–28 (2004).
16. Donehower, L. A. et al. Mice deficient for p53 are developmentally normal but susceptible to spontaneous tumours. *Nature* **356**, 215–221 (1992).
17. Jacks, T. et al. Tumor spectrum analysis in p53-mutant mice. *Curr. Biol.* **4**, 1–7 (1994).
18. Indra, A. K. et al. Temporally-controlled site-specific mutagenesis in the basal layer of the epidermis: comparison of the recombinase activity of the tamoxifen-inducible Cre-ER^T and Cre-ER^{T2} recombinases. *Nucleic Acids Res.* **27**, 4324–4327 (1999).
19. Soriano, P. Generalized lacZ expression with the ROSA26 Cre reporter strain. *Nature Genet.* **21**, 70–71 (1999).
20. Kemp, C. J., Wheldon, T. & Balmain, A. p53-deficient mice are extremely susceptible to radiation-induced tumorigenesis. *Nature Genet.* **8**, 66–69 (1994).
21. Collado, M. et al. Tumour biology: senescence in premalignant tumours. *Nature* **436**, 642 (2005).
22. Lowe, S. W. & Sherr, C. J. Tumor suppression by Ink4a-Arf: progress and puzzles. *Curr. Opin. Genet. Dev.* **13**, 77–83 (2003).
23. Xue, W. et al. Senescence and tumour clearance is triggered by p53 restoration in murine liver carcinomas. *Nature advance online publication*, doi:10.1038/nature05529 (24 January 2007).
24. Zhang, L. et al. Wild-type p53 suppresses angiogenesis in human leiomyosarcoma and synovial sarcoma by transcriptional suppression of vascular endothelial growth factor expression. *Cancer Res.* **60**, 3655–3661 (2000).
25. Teodoro, J. G., Parker, A. E., Zhu, X. & Green, M. R. p53-mediated inhibition of angiogenesis through up-regulation of a collagen prolyl hydroxylase. *Science* **313**, 968–971 (2006).
26. Dickins, R. A. et al. Probing tumor phenotypes using stable and regulated synthetic microRNA precursors. *Nature Genet.* **37**, 1289–1295 (2005).
27. Christophorou, M. A. et al. Temporal dissection of p53 function *in vitro* and *in vivo*. *Nature Genet.* **37**, 718–726 (2005).
28. Christophorou, M. A., Ringshausen, I., Finch, A. J., Swigart, L. B. & Evan, G. I. The pathological response to DNA damage does not contribute to p53-mediated tumour suppression. *Nature* **443**, 214–217 (2006).
29. Vassilev, L. T. et al. *In vivo* activation of the p53 pathway by small-molecule antagonists of MDM2. *Science* **303**, 844–848 (2004).
30. Haupt, S. & Haupt, Y. Manipulation of the tumor suppressor p53 for potentiating cancer therapy. *Semin. Cancer Biol.* **14**, 244–252 (2004).
31. Olive, K. P. et al. Mutant p53 gain of function in two mouse models of Li-Fraumeni syndrome. *Cell* **119**, 847–860 (2004).

Supplementary Information is linked to the online version of the paper at www.nature.com/nature.

Acknowledgements We thank N. Willis for helping to generate the LSL mice, H. Zheng for imaging mice, G. Wojtkiewicz for generating the movies with three-dimensional reconstruction, D. Crowley for help with histology, R. Bronson for reviewing the pathology, and M. Hemann for suggestions. A.V. is grateful to D. Ventura and G. Terranova for continuous support and encouragement. This work was supported by the Howard Hughes Medical Institute (T.J.), NCI (T.J., R.W., D.G.K.), and partially by a Cancer Center Support grant from the NCI (M.I.T.), the American Italian Cancer Research Foundation (A.V.), and the Leaf fund (D.G.K.). T.J. is the David H. Koch Professor of Biology and a Daniel K. Ludwig Scholar. D.A.T. is a Rita Allen Foundation Scholar.

Author Contributions A.V., D.G.K. and T.J. designed the experiments and wrote the paper. D.T. generated the p53-LSL mice and M.E.M. generated and characterized the Cre-ERT^{T2} mice, determined the optimal Tamoxifen dosage, assisted with histopathological analysis and commented on the manuscript. A.V., D.G.K. and L.L. derived and characterized the tumour cell lines. A.V. performed the immunostainings, the TUNEL assays the SA-β-Gal stainings and the western blottings. A.V., D.K. and L.L. performed the tamoxifen intraperitoneal injections. E.E.R. derived the MEFs. L.L. and J.N. maintained the mouse colony and genotyped the animals. J.G. and D.G.K. evaluated the magnetic resonance images, J.G. supervised the magnetic resonance imaging, generated the three-dimensional reconstructions and determined tumour volumes. R.W. optimized *in vivo* imaging protocols, reviewed imaging data, discussed the results, and commented on the manuscript.

Author Information Reprints and permissions information is available at www.nature.com/reprints. The authors declare no competing financial interests. Correspondence and requests for materials should be addressed to T.J. (tjacks@mit.edu).